ELSEVIER

Chemical Engineering Journal 84 (2001) 367–379

Chemical Engineering Journal

www.elsevier.com/locate/cej

A comprehensive model for the pressure drop in vertical pipes and packed columns

Geert F. Woerlee*, Joop Berends, Zarko Olujic, Jan de Graauw

Laboratory for Process Equipment, Delft University of Technology, Leeghwaterstraat 44, NL-2628 CA Delft, The Netherlands

Received 4 January 1999; received in revised form 4 December 2000; accepted 6 December 2000

Abstract

A macroscopic approach is used to describe the hydrodynamics of a two-phase annular counter-current flow in inclined flow channels. This type of flow is characteristic for gas–liquid contact equipment as applied in packed columns. In this study, a distinction is made between the pressure drop caused by the geometry of the channels and the pressure drop caused by the friction on the gas–liquid interface. It is shown that the frictional forces on the interface have two components that either influence the liquid interface velocity or induce waves on the interface. Special attention is paid to the description of the gas–liquid interaction. The interaction is described using an additional term on a undisturbed counter-current flow using a dimensionless expression. A set of three independent equation is derived, describing the liquid hold-up, the interface velocity and the different contributions to pressure drop as function of physical properties of both phase. The description is demonstrated on vertical pipes and packed columns containing either random or structured packing. Because of the general description, it is possible to predict the by liquid hold-up and pressure drop induced flood point in this equipment.

Keywords: Pressure drop; Gas–liquid interaction; Vertical tubes; Packed columns

1. Introduction

Due to the complicated nature of the counter-current gas–liquid-flow, earlier studies on packed column hydraulics have been mostly limited to correlating the experimental data. Newest correlations for the prediction of pressure drop, liquid hold-up, and flooding in packed columns are surveyed in Kister's book on the design of distillation columns [1]. Although some of the described methods do incorporate sound physical basis, there exists little generality among them.

The interaction between a falling film and a counter-current gas stream, appearing in equipment as wetted wall columns, falling film evaporators and reflux condensers, have been the subject of many thorough studies [2–4]. Zabaras and Dukler [5] reported that the models proposed in literature for flooding have been not so successful, because of the lack of detailed measurements needed for the evaluation of the physical mechanisms that control the process. Their experimental effort, which included measurements of the liquid distribution at up- and down-flow along with the time-dependent measurements of local film thickness and pressure gradient, gave a somewhat different picture than drawn previously [6]. Anyhow, new questions arose and other speculations concerning the gas–liquid interaction appeared requiring further investigations.

Kaiser [7], who considered the liquid-flow in a packed bed as a free surface gravity flow influenced by the upward flowing gas, has demonstrated that a more phenomenological approach to correlate experimental data could be rewarding, if fully explored. In response to this, we try to investigate the limits of a macroscopic approach to describe the hydrodynamics of a two-phase counter-current flow in a packed bed consisting of a number of inclined flow channels. In these channels, annular flow is assumed and interface friction and form drag are taken into account. Closing the relations with the necessary boundary conditions a set of four equations is obtained that permits prediction of liquid hold-up and pressure drop in packed columns containing either random or structured packing. Special attention is paid to the determination of the gas–liquid interaction, since this has turned out to be the key to a successful description of the two-phase flow behaviour and the description of the mass transfer in a packed bed (see [8]).

The determination of the gas–liquid interaction is also important to predict the flood point in packed beds. Hutton et al. [9], postulated that at least two types of liquid-flow instability can occur to initiate flooding, depending on the

* Corresponding author. Tel.: +31-20-419-6050; fax: +31-20-419-6051.
E-mail address: geert@feyecon.com (G.F. Woerlee).

1385-8947/01/$ – see front matter
PII: S1385-8947(01)00132-2

Nomenclature

a_p	specific packing surface area (m^2/m^3)
D_{col}	column diameter (m)
F_A	coefficient describing the gas–gas interaction
F_l	laminar coefficient of the packing friction
f	smooth pipe friction factor
f_g	geometrical friction factor
f_p	friction factor of the packing
f_p^*	friction factor of packing corrected for column diameter
f_∞	friction factor of packing at "infinite" flow rate
g	absolute gravitational acceleration (m/s^2)
Ga_p	packing Galileo number $Ga_p = 4\,\Delta\rho\rho_L g\cos\alpha/3\,\eta_L^2 a_p^3$
H_{col}	column height (m)
h	film thickness (m)
h_L	liquid hold-up ($h_L = a_p h$) (m^3/m^3)
h_0	free falling film thickness (m)
l_e	effective channel length in structured packing (m)
r	radial co-ordinate (m)
r_{int}	interface radius (m)
r_0	hydraulic radius (m)
Re_G	gas phase Reynolds number $Re_G = ((\rho_G(u_{SG}/\theta^2\varepsilon_0\cos\alpha) - u_{int})2\,\theta r_0)/\eta_G$
Re_L	liquid phase Reynolds number $Re_L = 4\,\rho_L u_{SL}/\eta_L a_p$
Re_p	packing Reynolds number $Re_p = Re_G\cos\alpha$
u_{int}	interface velocity (m/s)
u_G	gas velocity (m/s)
u_L	liquid velocity (m/s)
u_{SG}	superficial gas velocity (m/s)
u_{SL}	superficial liquid velocity (m/s)
z	axial co-ordinate (m)

Greek symbols

α	effective inclination angle (°)
α_0	effective inclination angle at infinite column diameter (°)
$\Delta\rho$	density difference (kg/m^3)
$\partial p/\partial z$	pressure drop over packed bed ($\partial p/\partial z = \partial p_f/\partial z + \partial p_g/\partial z$) (Pa/m)
$\partial p_f/\partial z$	frictional pressure drop (Pa/m)
$\partial p_g/\partial z$	geometrical pressure drop (Pa/m)
ε_{irr}	irrigated bed porosity (m^3/m^3)
ε_0	void fraction (m^3/m^3)
η_G	dynamic gas viscosity (Pa s)
η_L	dynamic liquid viscosity (Pa s)
θ	relative interface position ($\theta = r_{int}/r_0$)
ρ_G	gas density (kg/m^3)
ρ_L	liquid density (kg/m^3)
σ	surface tension (N/m)
ψ_{G-L}	gas–liquid interaction parameter

effective voidage of the packed bed. The first type, observed in conventional random packing, is due to interaction between the liquid hold-up and pressure gradient. The second is entrainment flooding, that is caused by wave type instability as encountered in wetted wall columns. In an other study [10], this second type of flooding is analysed. In this paper, it is shown that when applying an accurate model for the pressure drop, it is possible to predict the flood point caused by the liquid hold-up and pressure drop.

2. Macroscopic description of the flows

The geometry of a packed bed with a given porosity can be considered as a multiplicity of flow ducts consisting of a number, serially connected tubes. To keep the analysis simple, it is assumed that the steady state is maintained and that the liquid is residing in a laminar film of uniform thickness, totally wetting the channel walls.

2.1. Solution of the equation of motion for liquid-flow

The flow model taken here as basis for the further development is essentially that proposed by, e.g. Brauer [11], Hikita and Ishimi [12], for wetted wall columns, with laminar annular liquid-flow and a central gas flow. The average velocity profile of a counter-current flow in a tube with radius r_0 is shown in Fig. 1.

The interface is located at a distance r_{int}, which is the actual radius of the gas flow channel. Since the flow has axial symmetry, the velocity vector is dependent on the radial component r only. Then, the Navier Stokes momentum equation for a Newtonian incompressible liquid with viscosity η_L and density ρ_L moving in the gravitational direction

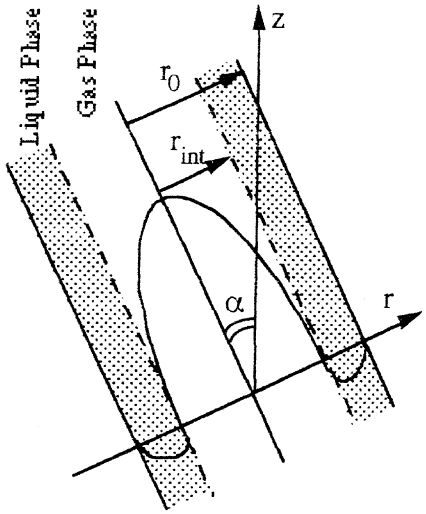

Fig. 1. Velocity profile of a counter-current liquid and gas flow in a tube.

enclosed by a gas with density ρ_G reduces to

$$0 = -\left(\Delta\rho g + \frac{\partial p}{\partial z}\right)\cos\alpha + \eta_L\left[\frac{1}{r}\frac{\partial}{\partial r}\left(r\frac{\partial u_L}{\partial r}\right)\right] \quad (1)$$

where u_L is the velocity, $\Delta\rho$ the density difference between the two phases and α represents the angle of the flow with the direction of gravity. In this study, the absolute gravitational acceleration is used $|g|$ and its direction is taken into account by using a negative sign. The pressure drop in the axial direction $\partial p/\partial z$ over an arbitrary structure, comprises frictional resistance and geometric resistance or form drag,

$$\frac{\partial p}{\partial z} = \frac{\partial p_f}{\partial z} + \frac{\partial p_g}{\partial z} \quad (2)$$

and will be in general, but not necessarily negative as well. The geometrical resistance is equal to zero when only straight tubes are considered. However, it contributes substantially when there are obstructions or bends in the gas flow as in a packed bed. The boundary conditions for Eq. (1) are

$$\text{for} \quad r = r_0: \quad u_L = 0 \quad (3a)$$

$$\text{for} \quad r = r_{int}: \quad u_G = u_L = u_{int} \quad \text{and} \quad \eta_G\frac{\partial u_G}{\partial r} = \eta_L\frac{\partial u_L}{\partial r} \quad (3b)$$

where u_{int} represents the interfacial velocity. The core and annular flows are distinguished by the subscripts G and L. It is convenient to generalise the calculations by introducing a dimensionless interface radius as

$$\theta = \frac{r_{int}}{r_0}. \quad (4)$$

Using the boundary condition (Eq. (3a)) in the differential Eq. (1), the liquid velocity is found as function of the radial co-ordinate as

$$u_L(r) = \frac{r^2 - r_0^2}{4\eta_L}\left(\Delta\rho g + \frac{\partial p}{\partial z}\right)\cos\alpha + \left[\frac{(1-\theta^2)r_0^2}{4\eta_L}\left(\Delta\rho g + \frac{\partial p}{\partial z}\right)\cos\alpha + u_{int}\right] \times \left(\frac{\ln(r/r_0)}{\ln\theta}\right). \quad (5)$$

After integration and dividing by the total area (πr_0^2), this yields the following expression for the superficial liquid velocity u_{SL}:

$$u_{SL} = -\frac{(1-\theta^2)^2}{8\eta_L}\left(\Delta\rho g + \frac{\partial p}{\partial z}\right)\cos\alpha r_0^2 - \left[\frac{(1-\theta^2)r_0^2}{4\eta_L}\left(\Delta\rho g + \frac{\partial p}{\partial z}\right)\cos\alpha + u_{int}\right] \times \left(\theta^2 + \frac{1-\theta^2}{2\ln\theta}\right). \quad (6)$$

The superficial liquid velocity, which normally is negative, is used as an input condition. To solve the boundary condition at the interface, one uses a force balance over the core gas flow at the interface. This allows us to write the shear stress of the gaseous phase at the interface as

$$\frac{1}{\cos\alpha}\eta_G\left.\frac{\partial u_G}{\partial r}\right|_{r=r_{int}} = \frac{\partial p_f}{\partial z}\frac{\theta r_0}{2}. \quad (7)$$

Here the frictional pressure drop is taken along the flow direction. This choice increases the distance and, therefore, the frictional pressure drop in the gravitational direction by a factor of one over $\cos\alpha$. Using Eq. (7) for the gas flow shear stress and the derivative of the liquid velocity at the interface (Eq. (5)), the shear stress interface condition (Eq. (3b)) can be solved, so that the interfacial velocity can be isolated as

$$u_{int} = -\left[\theta^2\ln(\theta)\left(\Delta\rho g + \frac{\partial p}{\partial z}\right)\cos\alpha + \frac{1-\theta^2}{2}\left(\Delta\rho g + \frac{\partial p}{\partial z}\right)\cos\alpha\right]\frac{r_0^2}{2\eta_L}. \quad (8)$$

Here relation (2) between friction pressure drop, geometrical and total pressure drop has been used to eliminate the frictional pressure.

2.2. The liquid hold-up

Before describing the pressure drops, the approach based on pipe flow needs to be adapted for an arbitrary structure, a packed bed. Therefore, the specific surface area a_p and the porosity of the packing ε_0 are related to a hydraulic radius as

$$r_0 = \frac{2\varepsilon_0}{a_p}. \quad (9)$$

The relative liquid hold-up (h_L) of a packed bed can be expressed as the liquid film thickness multiplied by the specific surface area. The liquid film thickness in a radial pipe is expressed as $h = 0.5(1-\theta^2)r_0$. Finally, the irrigated porosity is equal to the normal porosity minus the relative liquid hold-up

$$\varepsilon_{irr} = \varepsilon_0 - h_L = \varepsilon_0 - a_p h = \varepsilon_0 - a_p\tfrac{1}{2}(1-\theta^2)r_0 = \varepsilon_0\theta^2, \quad (10)$$

and, therefore, is a simple function of the dimensionless radius and the normal porosity of the packing.

2.3. Frictional pressure drop

As already mentioned, in a packed bed, the pressure drop is generally caused by a combination of frictional resistance and the geometric resistance. The frictional pressure drop can be expressed as function of a friction factor f in a tube and the velocity differences as

$$\frac{\partial p_f}{\partial z} = -\frac{f}{\cos\alpha}\frac{\rho_G\left(\frac{u_{SG}}{\varepsilon_0\theta^2\cos\alpha} - u_{int}\right)\left|\frac{u_{SG}}{\varepsilon_0\theta^2\cos\alpha} - u_{int}\right|}{\theta r_0} \quad (11)$$

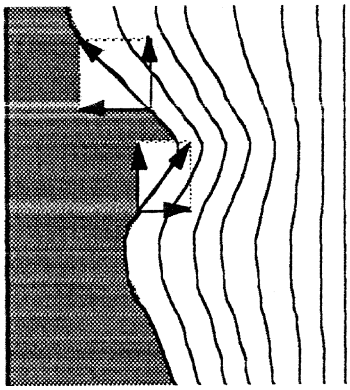

Fig. 2. The friction on the interface, illustrating that the area averaged forces on the flow must equal zero.

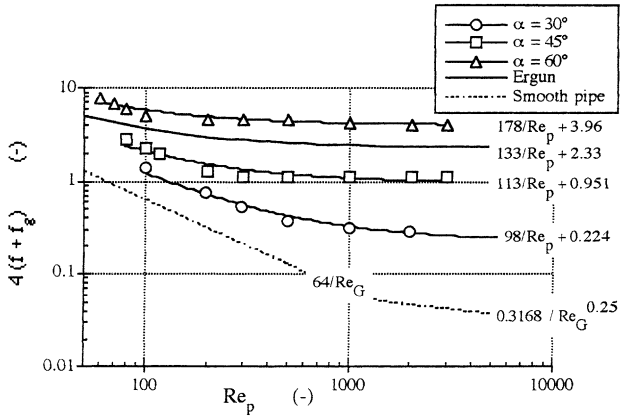

Fig. 3. The packing friction factor as function of the Reynolds number for structured packing with different angles, for the Ergun relation and for a smooth vertical pipe. The structured packing data are fitted with a relation similar to the Ergun relation.

where u_{SG} represents the superficial gas velocity, which is also used as input condition. Here, as well as in the case of the liquid phase, the superficial velocity is related to the cross-section area of the column. In the column, the actual gas velocity in the channels is obtained by dividing the superficial gas velocity by the irrigated bed porosity ($\varepsilon_0\theta^2$) and $\cos\alpha$. For a smooth interface, the Blasius equation can be applied to estimate the friction factor of a turbulent flow

$$4\,f = 0.3168\,Re_G^{-0.25} \tag{12}$$

where the gas flow Reynolds number is defined as

$$Re_G = \frac{\rho_G|(u_{SG}/\varepsilon_0\theta^2\cos\alpha) - u_{int}|2\,\theta r_0}{\eta_G}. \tag{13}$$

Both the gas load and the liquid load will influence the state of the interface, which will result in a wavy rather than a smooth interface. The consequence of this wavy interface is an increase of the radially directed shear stresses (see, Fig. 2), which are directed perpendicular to the flow. Since the interface has to remain unbroken, every force on the interface has to be compensated with a reaction force. Therefore, the average of the radially directed shear stresses are, when integrated over time or when integrated over the total surface area, necessarily equal to zero. As a consequence, there is no other force directed parallel with the liquid-flow than the force described by smooth pipe flow. However, since the energy losses are related to the square of the actual velocities, the wavy interface will cause an additional pressure drop in the gas phase. This additional pressure drop will be analysed in the section describing the gas–liquid interaction.

2.4. Geometrical pressure drop

The geometrical component of the pressure drop does not affect the liquid film directly and is largely a term that expresses the amount of work done by the gas to overcome all changes in flow directions and other kinds of form drag. The Ergun equation relates the friction factor of a random packed bed to it's Reynolds number Re_p. The relation can be reformulated as

$$\begin{aligned} 4\,f_p &= 4(f + f_g) = 4\left|\frac{\partial p}{\partial z}\right| \frac{\theta r_0}{\rho_G((u_{SG}/\varepsilon_0\theta^2) - u_{int}\cos\alpha)^2} \\ &= \frac{600}{9}\frac{\eta_G}{\rho_G((u_{SG}/\varepsilon_0\theta^2) - u_{int}\cos\alpha)\theta r_0} + \frac{28}{12} \\ &= \frac{133}{Re_p} + 2.33 \end{aligned} \tag{14}$$

where both the frictional and the geometrical term is included. The relation takes into account all possible pressure drops contributions, it is, therefore, likely that its general form can be used to describe other types of packed beds. The only difference in the Reynolds number for the tube and for the packing is the cosine term. They are simply related as $Re_p = Re_G\cos\alpha$.

Zogg [13] measured the pressure drops of corrugated sheets with smooth unperforated surfaces and different inclinations of the flow channels and extrapolated his results for limited geometries to an infinitely wide geometry to eliminate wall effects. Fig. 3 shows these extrapolated results as friction factors, together with the Ergun relation and the friction factor of a smooth pipe. The characteristic coefficients were obtained by fitting the experimental data using a Ergun type relation

$$4\,f_p = \frac{4\,F_1}{Re_p} + 4\,f_\infty \tag{15}$$

where f_∞ represents the friction coefficient at infinite Reynolds number and F_1 represents the laminar coefficient of the friction. Fig. 3 shows that the friction factor of a packed bed can in general be represented by Eq. (15).

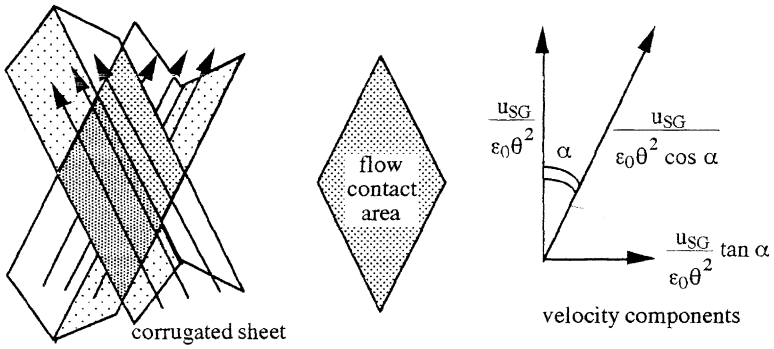

Fig. 4. Schematic view of the gas flow in corrugated sheets. Indicated are the contact area of the flow and the velocity components.

2.5. The effective inclination angle

To generalise the results on the inclination angle of the flow, it is necessary to interpret the obtained coefficients shown in Fig. 3. Therefore, we have illustrated the macroscopic gas flows within corrugated sheets in Fig. 4.

If first, the friction losses in a laminar flow are considered, it is noticed that they are fully caused by the shear stress with the walls. This means that the geometrical influence in the laminar coefficient is caused by the increase of the distance that the fluid travels through the packing. By multiplying the laminar coefficient by $\cos\alpha$, a channel friction factor should result, which is independent of the inclination angle. This is indeed the case as is shown in Fig. 5A.

The laminar friction coefficient has two natural boundaries given by the possible extreme values for a closed geometry, which are the cylindrical geometry, corresponding with a value of 64, and a rectangular or parallel plate geometry, corresponding with a value of 96. Fig. 5A shows that an average value of 83.5 is found for this coefficient and that the data points are within the given boundaries.

The infinite friction coefficient f_∞ covers the fully turbulent flow region, and is strongly effected by the open contact area of the gas flows within the packing structure. In this area, the radial component of the meeting gas flows is opposite, causing a rotation in the flow with a subsequent increase of the turbulence. Since the friction is related to the square of the velocity component the friction factor should be proportional to the square of the tangent of the inclination angle (see, Fig. 4). It is again noticed that the flow path for the gas in the corrugated sheets, and so the friction, is still increased by the increased path length as one over $\cos\alpha$. Finally, the infinite friction factor for a single phase flow can be expressed as

$$4\,f_\infty = \frac{0.6556\tan^2\alpha + 0.0142}{\cos\alpha}. \tag{16}$$

Here the constant 0.0142 represents the infinite friction

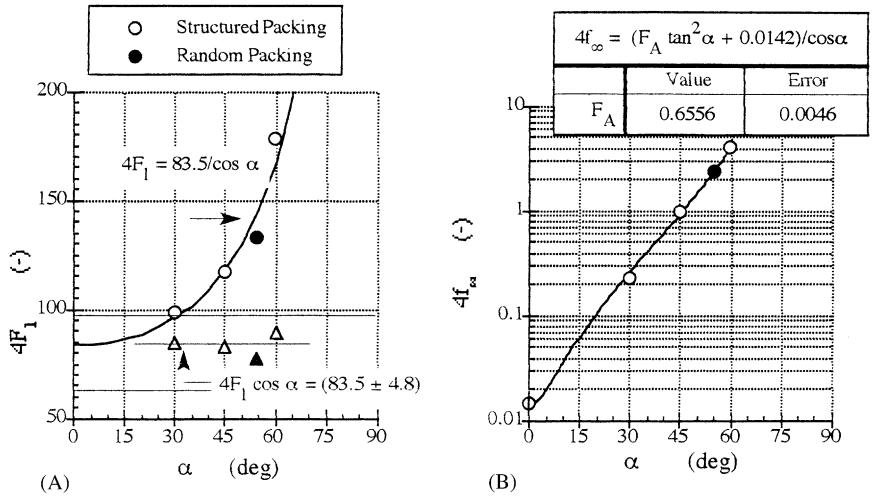

Fig. 5. (A) The laminar part of the packing structure as function of the effective packing angle, with its natural boundaries for a cylindrical (64/*Re*) and parallel plate (96/*Re*) geometry. (B) The graph shows the friction factor at infinite Reynolds number as function of the effective packing angle. The random packing parameters are obtained from the Ergun relation.

factor for a smooth pipe geometry, which value is derived by fitting the smooth pipe friction with relation (15). The constant 0.6556 is fitted with the data points. Fig. 5B shows that the behaviour of the infinite friction factor is described well by relation (16). The pressure drop over a non-irrigated packed bed, therefore, can be written as

$$\frac{\partial p}{\partial z} = -f_{\mathrm{p}} \frac{\rho_{\mathrm{G}}(u_{\mathrm{SG}}/\varepsilon_0)|u_{\mathrm{SG}}/\varepsilon_0|}{r_0} \tag{17a}$$

where the packed bed friction factor is expressed as

$$4\, f_{\mathrm{p}} = \left(\frac{83.5}{Re_{\mathrm{p}} \cos\alpha} + \frac{0.6556 \tan^2\alpha + 0.0142}{\cos\alpha} \right). \tag{17b}$$

This equation defines an effective inclination angle for a packing geometry relative to the Zogg data. The effective inclination angle is found by using dry pressure drop data. When Eq. (16) is applied using the value of 2.33 as given by the original type Ergun coefficient, a characteristic effective inclination angle of 54.9° is found for random packing. When the laminar part of the friction factor is used, an effective inclination angle of 51.1° is found. Since the friction factor at large, Reynolds numbers is much more sensitive to the inclination angle, the best procedure to determine the effective inclination angle is by measuring the infinite friction factor.

2.6. The influence of the column diameter on the pressure drop

Especially for small columns with a diameter less than 1 m, it has been observed that pressure drop varies with column diameter [1]. In randomly packed columns, it increases and in regularly packed columns it decreases with increasing diameter. Since the diameter can have a large influence on the pressure drop and, therefore, on the determined effective inclination angle, it is necessary to address this effect and adjust the main equations.

The pressure drop decrease with increasing diameter in structured packing is due to the channel endings at the wall. When the gas flow reaches the wall, it has to change its direction by an angle of 2α. This effect can be compared with a bend or elbow in the gas flow and it can, therefore, be expressed as an apparent increase of the channel length. This increase depends on the shape and angle of the turn and on the Reynolds number of the flow and is generally expressed in equivalent pipe diameters. By analysing, the standard tables on the pressure drop increase of bends and turns (see, e.g. [14]), it is found that the apparent pipe length increase, caused by a smooth turn in the flow direction can be approximated as $0.4 r_0$ times the angle of flow direction change. In a column with given diameter, D_{col} and height H_{col}, a total effective channel length for the fluid l_{e} is expressed as (see, Fig. 6)

$$l_{\mathrm{e}} = \left(\frac{(2/\pi) D_{\mathrm{col}}}{\sin\alpha} + 0.4\, r_0 2\alpha \right) \left(\frac{H_{\mathrm{col}} \tan\alpha}{(2/\pi) D_{\mathrm{col}}} \right). \tag{18}$$

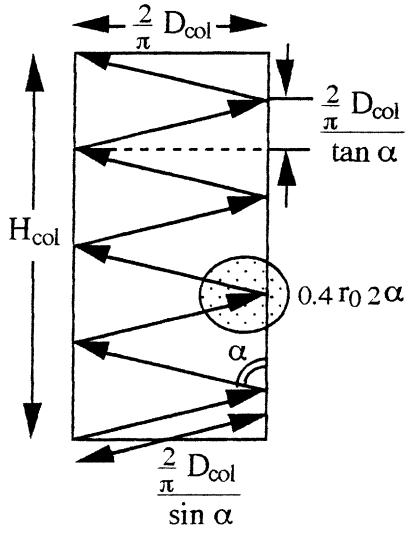

Fig. 6. The flow path in a with structured packing filled column. The average sizes used to calculate the column diameter influences on pressure drop are indicated.

Here the inclination angle is expressed in degrees, which varies from 0 to 90°. The diameter of the column is multiplied by the factor $2/\pi$, representing the average channel length within the column. This factor takes into account that the channels that are not going trough the centre of the column are shorter. The first right hand side term of Eq. (18) represents the unit length of a channel to the wall and the additional apparent length caused by the bend at the wall of the column. The second right hand side term represents the number of such channels over the height of the column. The apparent flow path length for the gas phase within the column per unit height can be expressed as

$$\frac{l_{\mathrm{e}}}{H_{\mathrm{col}}} = \frac{1}{\cos\alpha} \left(1 + \frac{2.5\, \varepsilon_0 \alpha \sin\alpha}{a_{\mathrm{p}} D_{\mathrm{col}}} \right)$$
$$\Rightarrow f_{\mathrm{p}}^{*} = f_{\mathrm{p}} \left(1 + \frac{2.5\, \varepsilon_0 \alpha \sin\alpha}{a_{\mathrm{p}} D_{\mathrm{col}}} \right), \tag{19}$$

so that the structured packing friction factor can be corrected for the column diameter effects. The cosine term is the increase in length for the gas phase and is taken already into account in Eq. (7) for the frictional pressure drop and in the relation (17) for the geometrical pressure drop. The right hand factor, therefore, remains as correction for the effect of the column diameter.

Since in random packing, there is no well defined flow channel, the flow is not exclusively forced to turn direction at the end of the wall, but it will consider the wall as just another, in this case, vertical packing element. In smaller diameter columns, the presence of the wall is felt more, causing a more vertical directed flow and, therefore, a smaller effective inclination angle for the packing. The effective angle of the column will become the ratio of available packing area and the total area, including the wall of

the column. Adding the two area weighted angles leads to

$$\frac{\alpha}{\alpha_0} = \frac{a_p(\pi/4)D_{col}^2}{a_p(\pi/4)D_{col}^2 + \pi D_{col}} = \frac{1}{1 + (4/a_p D_{col})} \quad (20)$$

where α_0 is the effective inclination angle at infinite column diameter. With Eqs. (19) and (20), the effect of the column diameter can be estimated.

2.7. Gas–liquid interaction

As stated above, it can be assumed that the increasing velocity difference of the two phases, leads to a number of effects on the liquid film. The interface will first become increasingly wavy, after which the gas entrains droplets and finally forces the liquid film upwards. These effects will lead to an increase of the pressure drop, which represents the extra energy dissipation in the gas phase. Therefore, the pressure drop of the packed bed is written as a non-disturbed pressure drop multiplied with a correction for the gas–liquid interaction

$$\frac{\partial p}{\partial z} = -f_p(1 + \psi_{G-L}) \times \frac{\rho_G \left(\frac{u_{SG}}{\theta^2 \varepsilon_0} - u_{int}\cos\alpha\right)\left|\frac{u_{SG}}{\theta^2\varepsilon_0} - u_{int}\cos\alpha\right|}{\theta r_0}. \quad (21)$$

Here ψ_{G-L} represents the change of the friction factor due to the interaction of the gas and liquid phase. The liquid hold-up has an important influence on the gas–liquid interaction. To describe the hold-up influence it is compared with the undisturbed situation for the liquid-flow. When a free falling film with a thickness (h_0) is multiplied with the specific surface area, two characterise dimensionless numbers are found, expressing the undisturbed liquid hold-up

$$a_p h_0 = a_p \left(\frac{3\rho_L}{\rho_L \Delta\rho g \cos\alpha}\frac{\rho_L |u_{SL}|}{a_p}\right)^{0.33} = \left(\frac{3\eta_L^2 a_p^3}{4\rho_L \Delta\rho g \cos\alpha}\frac{4\rho_L|u_{SL}|}{a_p\eta_L}\right)^{0.33} = (Ga_p^{-1}Re_L)^{0.33}. \quad (22)$$

Here Re_L is the liquid Reynolds number and Ga_p represents a Galileo number for the packing. Eq. (22) has the advantages that the film thickness is represented by a dimensionless number depending on the liquid-flow and a dimensionless number that is depending only on the geometry and physical properties of the system.

The interaction of the gas and the liquid phase, is described using flow related dimensionless groups (Re_L, Re_G, θ) and dimensionless groups that are related to physical properties of the system (Ga_p, ρ_L/ρ_G, η_L/η_G). By analysing literature data [15,16], own data and comparing the results with pressure drop correlations given in literature (e.g. Feind [2], Teutsch [17], Hetsroni [6], Billet and Schultes [18]), the gas–liquid interaction parameter in counter-current flow was correlated as

$$\psi_{G-L} = \sinh\left[\frac{34\times10^{-15}(1-\theta^2)^7}{(\cos\alpha)^9 Re_L^2 Ga_p^{-2}} Re_L Re_G^{1.5}\frac{\rho_L\eta_L}{\rho_G\eta_G}\right] = \sinh\left[\frac{34\times10^{-15}}{(\cos\alpha)^9}\frac{a_p h}{\varepsilon_0^7}\left(\frac{h}{h_0}\right)^6 Re_L Re_G^{1.5}\frac{\rho_L\eta_L}{\rho_G\eta_G}\right]. \quad (23)$$

The sinus hyperbolic form is used because the friction factor in a pipe flow increases exponentially with increasing surface roughness (see, e.g. [19]). When either the gas or liquid-flow

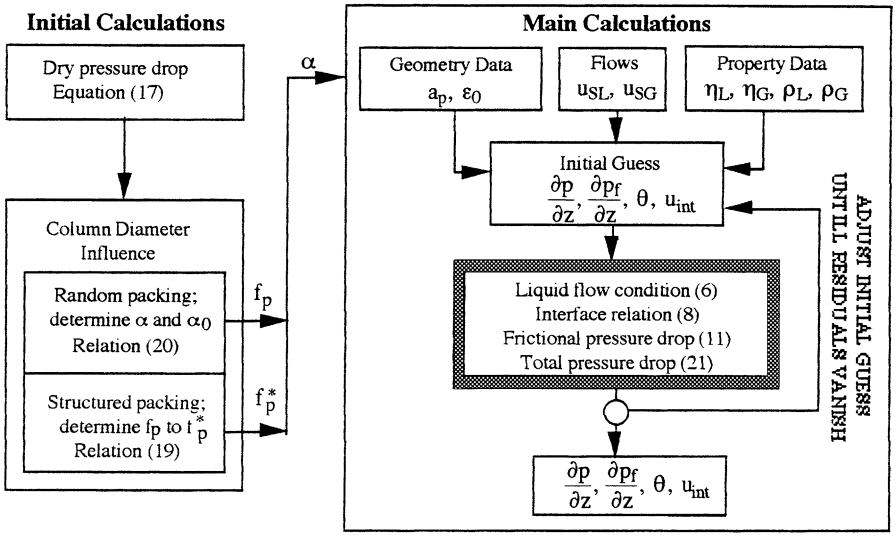

Fig. 7. Block diagram showing the calculation method for the implicit flow parameters and the secondary parameters as column diameter corrections and the effective inclination angle.

gets small, the gas–liquid interaction parameter of Eq. (23) becomes small as well and the undisturbed situation remains. In Section 2.8, the correlation will be tested using pressure drop in both random and structured packing. In an other study on mass transfer [8], it is shown that relation (23) can be connected with both the gas and liquid mass transfer coefficients.

2.8. Calculation procedure

At given liquid load, specified by Eq. (6), and given gas load, specified by Eq. (11), the film thickness, interface velocity, frictional pressure drop and total pressure drop have to be determined. These quantities can be solved using the velocity at the interface, expressed in Eq. (8), and the relations for the friction factor (12) and the total pressure drop (23). However, except for the liquid interface velocity, the parameters cannot be expressed explicitly, so that the relations are to be solved using an iteration procedure. The calculation is started using initial estimates for the variables mentioned and continues until a satisfactory agreement between the subsequently calculated values is reached. The calculation procedure, including the initial calculations, is shown in Fig. 7.

3. Results and discussion

Following the above strategy, it is possible to calculate all flow parameters. This is subsequently done for a number of different systems of which experimental data is available. Literature data are used to investigate and develop the model, while mainly own measurements are used for the validation. The physical properties and the properties of the packing structure are given in Appendix A for all configurations used.

3.1. The liquid hold-up

One of the key assumptions is the use of the smooth pipe interfacial friction to calculate the axial effects on the liquid film. Since this assumption, stated in Eqs. (11) and (12), directly affects the interfacial velocity, the assumption is verified by measuring the behaviour of the liquid hold-up as function of the gas velocity. The simplest geometry in which this can be verified, is the vertical pipe. Fig. 8 shows the predicted and measured [16] film thicknesses, as function of the gas load in a vertical pipe with inner diameter of 50.8 mm. The graph shows that the liquid hold-up is well predicted over the whole gas load range. The model predicts a small increase of the film thickness with increasing gas load.

Fig. 9A and B show the total liquid hold-up as function of the gas load for a column with structured gauze packing. The shape of the curve is predicted well over the whole range of gas throughput, validating the assumption that the parallel shear on the liquid film is approximately identical to the shear of a gas flow in a smooth pipe. The absolute deviations in these cases are most likely caused by the fact that a relatively small column diameter was used in combination with a gauze packing. This last fact could simply lead to an additional static hold-up in the packing structure and to a different flow angle for the gas and for the liquid-flow.

Finally, Fig. 10 shows the measured and predicted liquid hold-up for two commercial structured packings (Montz B series) as function of the superficial liquid mass velocity at zero gas velocity. The measurements were carried out on the test rig of the packing manufacturer at ambient conditions using water as liquid phase. The results support the idea of the laminar falling film within a packing structure. The lower hold-up values found at low liquid-flows are probably caused by insufficient wetting of the packing.

3.2. Specific area and column diameter

In the presented model, information on specific surface area, column diameter, etc. has been transformed to a channel diameter and an effective inclination angle for gas and liquid-flow. When the corrections for diameter influence are carried out an identical effective inclination angle should be found for similar packing types. Tables 1 and 2 show the results for the Montz B1 series as function of the specific surface area and column diameter.

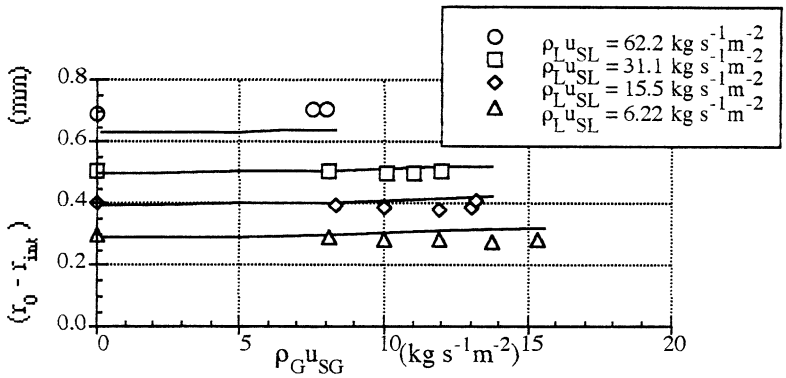

Fig. 8. The calculated and measured [16] liquid film thickness in a vertical pipe as function of the gas throughput for four liquid loads.

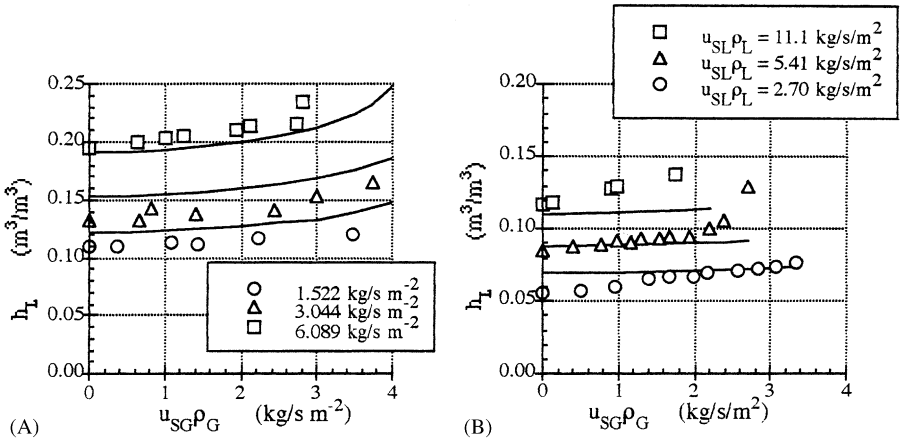

Fig. 9. (A) The measured (this study) and calculated hold-up for glycol–air system, as function of the gas throughput for structured gauze packing. (B) The measured (this study) and calculated hold-up for water–air system, as function of the gas throughput for metal sheet structured packing.

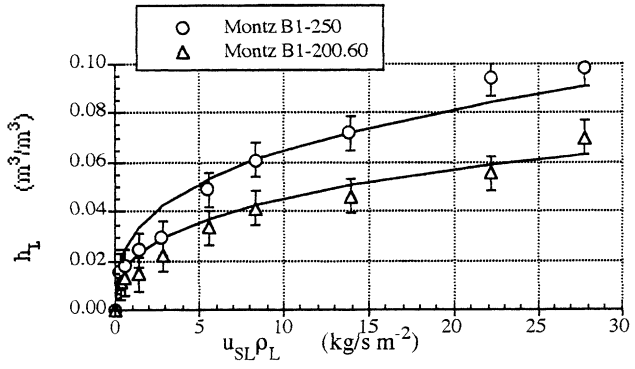

Fig. 10. A comparison of the measured (this study) and predicted relative volumetric liquid hold-up at zero gas load in a bed with corrugated sheet packing as function of the liquid load.

Table 1
The effect of the specific area of the packing on the effective inclination angle for a Montz B1 packing constructed at 45° and a 30°

a_p (m^2/m^3)	α (45° construction) (°)	α (30° construction) (°)
110	39.8	27.0
123	39.7	26.9
190	38.2	27.1
258	39.9	26.3

The tables show that the approach used to calculate the geometrical effects are valid. However, one should remain careful with the column diameter influence on the pressure drop, because effects like changes in space between packing and column wall, non-careful installation of the packing elements, etc. can ruin the effect of scale-up rules easily.

Table 2
The effect of the column diameter on the effective inclination angle for Montz B1–250

D (m)	α (45° construction) (°)
0.48	40.0
0.79	39.9
1.57	38.9
2.75	38.9

3.3. Vertical pipe pressure drop

The model is developed to predict pressure drops in packed beds. However, the model is based on the vertical pipe geometry and it, therefore, also should predict the correct pressure drop in this geometry. Besides this, it is an important test for the model, since the gas–liquid interaction parameter (ψ_{G-L}) in this geometry is most directly influencing the pressure drop. Fig. 11 shows a comparison of the pressure drops as calculated with the correlation given by Feind [2] and the pressure drop as calculated with the presented model. Taking into account that pressure drops are normally presented on a double logarithmic scale, the model results of this study compare reasonable well with the Feind correlation. The correlation of Feind is based on gas Reynolds numbers which are not taken relative towards the interface velocity, while the presented model takes the gas velocity relative to the interface velocity. The gas–liquid interaction parameter becomes close to zero for small liquid or gas Reynolds number. This means that the presented model especially leads to reliable pressure drop predictions for small liquid or gas loads. The deviations for large liquid Reynolds numbers are partly due to our liquid laminar flow model. However, the model remains predicting a larger pressure drop then the Feind correlation when applying a turbulent liquid-flow model.

3.4. Random packing pressure drop

Fig. 12 shows the comparison of predicted and measured pressure drops for a packed bed consisting of ceramic berl saddles. Since no direct dry pressure drop data were available, the pressure drops were calculated with the effective inclination angle found of the Ergun relation. An interesting

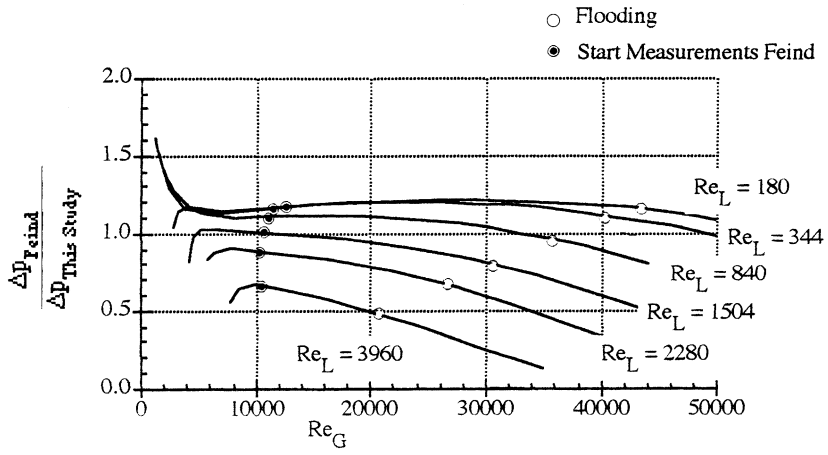

Fig. 11. The ratio of the calculated pressure drops according to Feind [2] and this study, as function of the gas Reynolds number for six liquid Reynolds numbers. The flooding points and the gas flow limits given by Feind are indicated.

result is the existence of two mathematically stable solutions for the pressure drop corresponding to two different liquid hold-ups. In a gas–liquid system, only the lower solution results in a stable counter-current film flow. However, the upper and lower stable pressure drops, more often represented as a small and a large hold-up of one phase, are found in liquid–liquid extractions. The stable configuration is then dependent on the start-up procedure. In other words, because of its generality, the proposed model is valid for other systems provided the flow is annular. Given that no exact data were used for the calculation of the effective inclination angle, the results are rather good. The model predicts the steep increase of the pressure drop before the flooding point relatively accurately.

Fig. 13 shows the calculated and measured pressure drops in a packed bed consisting of plastic pall rings. To determine the effective inclination angle use has been made of the dry pressure drop as measured by Krehenwinkel et al. [15]. The calculated pressure drops are within an accuracy of 10% of the measured values. The figure shows that the liquid-flow does not reach the end of the calculated pressure drop line and flooding occurs at an earlier stage. To our opinion, this indicates the second mechanisms for flooding, i.e. the entrainment of droplets in the gaseous phase, while Fig. 12 shows a system where flooding is determined by the friction of the gas on the liquid film. One could say that there is a macroscopic and a microscopic cause for the occurrence of flooding. Which of the two mechanism governs the flood point depends on the physical properties of the fluids and the packing characteristics.

3.5. Structured packing pressure drop

The prediction of the pressure drops of a structured packing at various gas and liquid loads using the given model are shown in Figs. 14 and 15 for the water–air system at

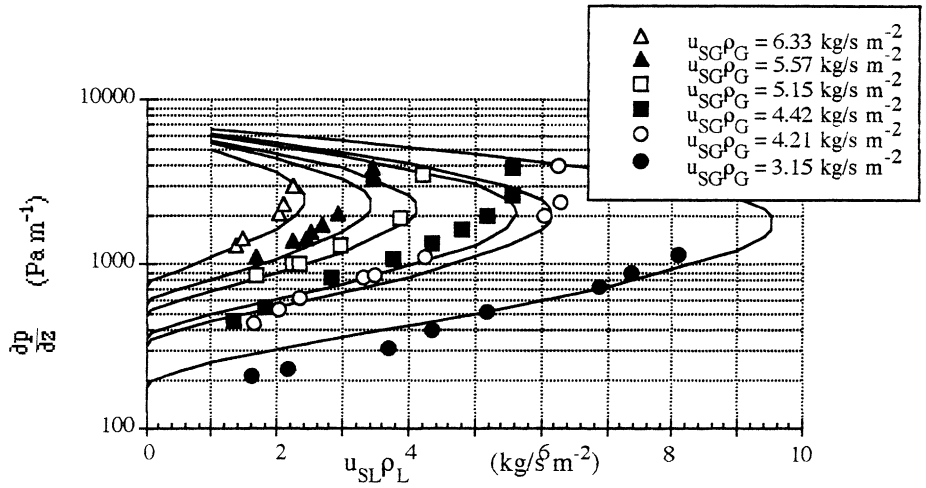

Fig. 12. The measured [15] and calculated pressure drops as function of the liquid load for various gas throughputs in a column with ceramic berl saddles.

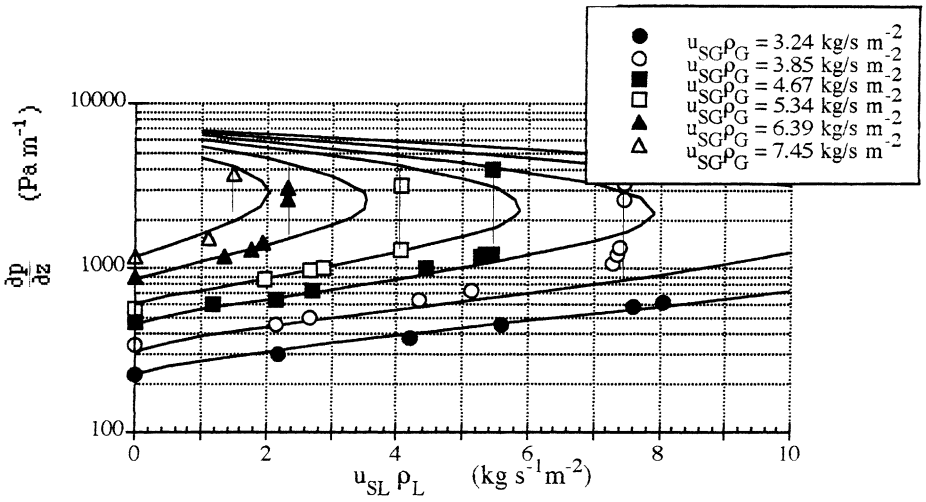

Fig. 13. The measured [15] and calculated pressure drops as function of the liquid load for various gas throughputs in a column with plastic pall ring.

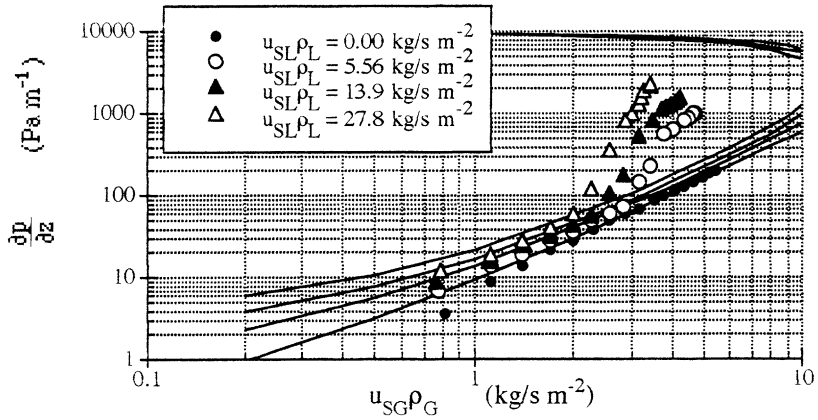

Fig. 14. The measured and calculated pressure drops as function of the gas throughput for three liquid loads and the dry pressure drop in a structured packing with an effective inclination angle of 26.3 and specific surface of 260 m^2/m^3 (see also Appendix A).

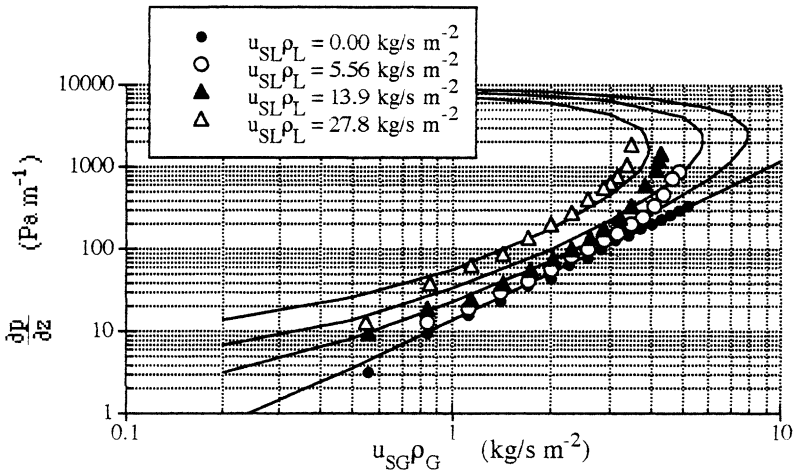

Fig. 15. The measured and calculated pressure drops as function of the gas throughput for three liquid loads and the dry pressure drop in a structured packing with an effective inclination angle of 39.9 and specific surface of 110 m^2/m^3.

ambient conditions, as measured in this study. Fig. 14 shows the measurements and calculations for a packing with an inclination angle of 30° and specific area of 260 m^2/m^3, while Fig. 15 shows the results for a packing with an inclination angle of 45° and a specific area of 110 m^2/m^3. Both figures show that the dry pressure drop can be described using the packing dimensions and an effective inclination angle. The liquid loads in both systems are relatively large. However, this firstly shows that the liquid-flow causes a non-zero pressure drop at zero gas velocity in the model, indicating that the gas is dragged down by the liquid-flow at the interface. The maximum deviations for systems with design angle of 45° were determined in the pre-loading range as +50%, while those for an angle of 30° were determined as +30%. The pressure drop increase caused by the loading in the packing is not predicted well for the packing with an inclination angle of 30°. The reason for this is most likely explained by the fact that the structured packing behaves as a demister. Droplets are recollecs by the on the liquid-flow film droplets.

4. Concluding remarks

A model has been presented that is able to describe two-phase film flow systems for various physical properties. The presented model is based on a laminar liquid film, which totally wets the packing. This idealised situation leads to deviations for structured packing pressure drop due to entrainment. Clearly, it is not possible to predict deviations from idealised behaviour with the presented model, but the model provides a tool to identify these deviations. This for instance means that wetting can be analysed by measuring the hold-up in the packing.

As already postulated by Hutton et al. [9], the pressure drop model revealed the existence of two principal flooding mechanisms, of which one is caused by the drag on the liquid film while the other mechanism has its base in the entrainment of droplets. Deviations of the measured and calculated pressure drops in the loading regime indicate a transitional state of counter-current flow with increasing entrainment. The comparison of the measured and calculated pressure drop in packings and vertical pipes showed that the used interaction description for the gas and the liquid could describe both the frictional as geometrical increase of the pressure drop. Since the increase of the gas–liquid friction is described well, it is also possible to predict the gas phase mass transfer coefficient in packed beds by using Chilton-Colburn like relation. In an other study [8], it is shown that next to the gas mass transfer coefficient, the liquid mass transfer coefficient is related to the gas–liquid interaction. The surface renewal of the liquid phase can be related to Eq. (23) using an energy balance and calculating the dissipated wave energy.

The model presented has a sound physical basis. However, the description of the gas–liquid interactions taking into account the increase of the surface roughness (relation (23)), is largely an empirical parameter. It has been tried to use the gas–liquid interaction parameter in a clear and unambiguous way and although it reasonably predicts the pressure drop, it can likely be improved.

Appendix A

The physical properties used to analyse the hydrodynamic relations. Next to the physical properties of the systems, the packing characteristics are shown together with the column diameter.

Reference	ρ_L (kg/m^3)	ρ_G (kg/m^3)	η_L (mPa s)	η_G (mPa s)	σ (N/m)	a_p (m^2/m^3)	ε_0 (m^2/m^3)	α (°)	D_{col} (mm)
Fig. 8	998	1.205	1.002	0.018	0.073	78.7	1.0	0.0	50.8
Fig. 9A	1090	1.205	8.1	0.018	0.048	650	0.98	29	38
Fig. 9B	998	1.205	1.002	0.018	0.073	580	0.96	38	38
Fig. 10 (top)	998	1.205	1.002	0.018	0.073	260	0.975	40	790
Fig. 10 (bottom)	998	1.205	1.002	0.018	0.073	190	0.978	27	790
Table 1	998	1.205	1.002	0.018	0.073	–	–	–	790
Table 2	998	1.205	1.002	0.018	0.073	260	0.975	–	–
Fig. 11	998	1.205	1.002	0.018	0.073	133	1.0	0.0	–
Fig. 12	830	27.39	1.393	0.015	0.027	303	0.59	56	155
Fig. 13	826	13.48	1.274	0.016	0.026	375	0.846	58.5	155
Fig. 14	998	1.205	1.002	0.018	0.073	260	0.975	26.3	790
Fig. 15	998	1.205	1.002	0.018	0.073	110	0.987	39.9	790

References

[1] H.Z. Kister, Distillation Design, McGraw-Hill, New York, 1992.
[2] K. Feind, Strömungsuntersuchungen bei Gegenstrom von Rieselfilmen und Gas in lotrechten Rohren, VDI-Forsch. Heft 481, Düsseldorf, 1960.
[3] G.B. Wallis, One-Dimensional Two-Phase Flow, McGraw-Hill, New York, 1969.
[4] H. Imura, H. Kusuda, S. Funetsu, Flooding in a counter-current annular two-phase flow, Chem. Eng. Sci. 32 (1977) 79–87.
[5] G. Zabaras, A.E. Dukler, D. Moalem-Maron, Vertical upward co-current gas–liquid annular flow, AIChE J. 32 (5) (1986) 829–843.

[6] G. Hetsroni, Handbook of Multi-phase Systems, Hemisphere, Washington, 1982.
[7] V. Kaiser, Flooding in Packed Columns Correlated Another Way, AIChE Spring National Meeting, March/April 1993, Houston (see also, Chem. Eng. Progr. 90 (6) (1994) 55–59).
[8] G.F. Woerlee, Hydrodynamics and Mass Transfer in Packed Columns and their Applications for Supercritical Separations, Delft University Press, Delft, 1997.
[9] B.E.T. Hutton, L.S. Leung, P.C. Brooks, D.J. Nicklin, On flooding in packed columns, Chem. Eng. Sci. 29 (1974) 493–500.
[10] G.F. Woerlee, J. Berends, A capacity model for vertical pipes and packed columns based on entrainment, Chem. Eng. J., (2001).
[11] H. Brauer, Widerstandsgesetze für innen berieselte und gasdurch strömte senkrechte Rohre, Chem. Ing. Technol. 32 (11) (1960) 719–725.
[12] H. Hikita, K. Ishimi, Frictional pressure drop for laminar gas streams in wetted-wall columns with co-current and counter-current gas–liquid, J. Chem. Eng. Jpn. 9 (1976) 351–362.
[13] M. Zogg, Strömungs- und Stoffaustauschuntersuchungen an der Sulzergewebepackung, Diss. No. 4886, Technische Hochscule Zürich, 1972.
[14] R.H. Perry, D.W. Green, Perry's Chemical Engineering Handbook, 6th Edition, McGraw-Hill, New York, 1984.
[15] H. Krehenwinkel, H. Knapp, Pressure drop and flooding in packed columns operating at high pressures, Chem. Eng. Tech. 10 (1987) 231–242.
[16] A.E. Dukler, L. Smith, A. Chopra, Flooding and upward film flow in tubes. Part I, Int. J. Multi-Phase Flow 10 (1984) 585–597.
[17] T. Teutsch, Druckverlust in Füllkörperschüttungen bei hohen Berieselungsdichten, Chem. Ing. Technol. 36 (5) (1964) 469–503.
[18] R. Billet, M. Schultes, Modelling of pressure drop in packed columns, Chem. Ing. Technol. 14 (1991) 89–95.
[19] W. Nunner, Wärmeübergang und Druckabfall in rauhen Rohren, VDI-Forsch, Heft 455, Düsseldorf, 1956.